

# Lithographically fabricated ultra-hydrophobic and porous plant-like surfaces for bio chip applications

O. Mertsch, A. D. Walter, D. Schondelmaier and B. Loechel

Berliner Elektronenspeicherringesellschaft für Synchrotronstrahlung m.b.H. (BESSY GmbH)  
- Applicationcenter for Microengineering (AZM) -  
12489 Berlin, Germany, mertsch@bessy.de

## ABSTRACT

A new and efficient way for the fabrication of ultra-hydrophobic and ultra-porous surfaces for bio chip and MEMS applications and for the production of nano-membranes is presented. This method is based on a back-side UV-exposure with some substantial changes in the exposure conditions. Plant-like structures of resist have been generated with wetting contact angles of about  $125^\circ$ . By applying additional layers such as self assembled mono layers (SAM) on thin metal films after the lithographic step, the contact angle could be increased of up to  $165^\circ$ . Due to the lithographic fabrication method, such surfaces can easily be integrated into micro fluidic channels via multi step exposures.

**Keywords:** wetting, contact angle, ultra-hydrophobic surfaces, back-side exposure, plant-like structures

## 1 INTRODUCTION

Since the middle of last century the wettability of surfaces has become of great interest to many different research fields and technical applications. First of all a very special surface morphology which leads to the so called "Lotus Effect" is of great importance for self cleaning products like paintings, glass panels for applications in cars and buildings and furthermore for biological and medical systems [1]. In such special cases ultra-hydrophobic surfaces with contact angles of more then  $150^\circ$  allow very interesting new solutions for MEMS and  $\mu$ -TAS applications.

The big advantage of this effect is the generation of micro drops and thus the minimization of the probe volume as well as the surface contact between the fluid and the solid walls. Hence, nonspecific adsorption mainly in biotechnology applications can be reduced drastically [2]. Because of the increasing surface to volume ratio, forces based on molecule interactions like hydrophilic bonding, van der Waals forces and capillary forces became the dominating parameters for drop volumes below  $10 \mu\text{L}$  [3].

The interaction of such small drops and the patterned surface enable a number of new and interesting possibilities for the transportation of micro drops. Interfacial tension

gradients are the new way of movement control on ultra-hydrophobic surfaces [4,5]. They can be achieved by creating changes in the surface tension underneath the drop.

The most important aspect for the whole drop fluidic and drop motion field is the availability of ultra-hydrophobic surfaces on which the fluidic samples form drops. That means contact angles of above  $150^\circ$  and very low contact angle hysteresis are necessary for sufficient drop transportation [8]. Such surfaces can be fabricated by different technical approaches [6-8] but there are always problems due to sticking effects so that not every surface is capable for drop motion experiments.

This paper presents a new way for creating ultra-hydrophobic surfaces with the demanded properties by a very simple back-side lithographic exposure [see also 9,10]. Big advantage of this technique is the creation of nanoporous structures and side walls within one lithographic step so that hydrophobic surfaces can be produced by the resist only. Furthermore, different layer techniques are presented which cause even more ultra-hydrophobic surfaces with very low hysteresis.

## 2 WETTING DYNAMICS

The first mathematical description of the wetting behavior of fluids on plane smooth surfaces was described by Thomas Young in 1805 who explained the drop shape as a result of the participating interfacial tensions ( $\gamma$ ) on the drop:

$$\cos \theta_0 = \frac{\gamma_{solid,vapor} - \gamma_{solid,liquid}}{\gamma_{liquid,vapor}} \quad (1)$$

The contact angle  $\theta_0$  (ca) is determined by the chemical nature of the solid and the three forces working on the contact line (triple point). The equation describes wetting of smooth surfaces very well but for ultra-hydrophobic surfaces, where the influence of roughness becomes more and more important, this equation is not longer sufficient to predict the real contact angle.

The wetting behavior of such surfaces can be described by two different states, both based on different assumptions concerning the penetration of the rough surface by liquids. The first one is the so called Wenzel case, first mentioned

in 1936 in which R.N. Wenzel described the surface roughness as the important factor for increasing the natural hydrophobicity of the material [11]. Based on this he stated that the real contact angle of such surfaces arises from multiplying the Young-angle with the roughness factor ( $r$ ):

$$\cos \theta_w = r \cos \theta_0 \quad (2)$$

where ( $r$ ) is given by the ratio of the true surface area and the apparent one and which is always bigger than 1. Equation (2) describes very well the behavior of hydrophilic surface ( $\theta_m < 90^\circ$ ) getting more hydrophilic and hydrophobic surfaces ( $\theta_m > 90^\circ$ ) getting more hydrophobic when patterned. But there are still observations which could not be described by this equation. Rolling up from super-hydrophobic surfaces for example cannot be explained by fluids which sink into the roughness like predicted by Wenzel.

For this reason A.B.D. Cassie and S. Baxter described in 1944 a second model in which the fluid contacts the solid only on the top of the structures and do not penetrate the space between them [12]. That is why this state is usually called the “fakir state”. In this case the increase in contact angle is caused by the decreasing contact area of the solid ( $f_1$ ) and the increasing area of air underneath the drop ( $f_2$ ):

$$\cos \theta_{CB} = f_1 \cos \theta_0 + f_2 \cos \theta_0 \quad (3)$$

The contact angle of the fluid with air is  $180^\circ$  and so an increasing air area underneath the drop changes the Cassie-Baxter contact angle to higher values.

### 3 METHODS

The wetting dynamics showed the importance of roughness and the surfaces structure for achieving ultra-hydrophobic behavior. For this reason we present a lithographic process with a back-side exposure step for creating plant-like surfaces with nano-porous sidewalls.

Figure 1 compares a standard contact UV-lithography and the back-side UV-lithography we used in this paper. The most important changes and premises we used in this process are the use of SU 8 as a negative resist matrix, the back-side exposure to connect the resist from the substrate side, a very low exposure dose between 30-200 mJ/cm<sup>2</sup>, and a resist thickness slightly thicker than the final structures.

As substrates we used boro-float glass substrates which were covered with SU 8 by spin coating. The final thickness of the resist was about 25  $\mu\text{m}$ . In these experiments, we use an UV mask with square structures and length scales reaching from 4  $\mu\text{m}$  to 12  $\mu\text{m}$ , and spaces between them reaching from 4  $\mu\text{m}$  to 120  $\mu\text{m}$ .

The metal thin films for the SAM coating were deposited by Argon-sputtering techniques directly on the patterned and post baked SU 8 resist. As SAM we used two

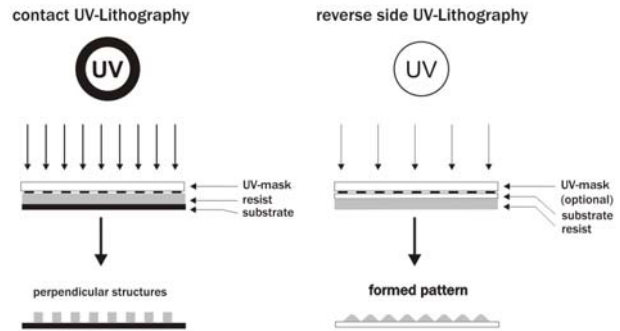


**Figure 1:** Comparison of a standard contact lithography and the back-side exposure with a reduced dose. The transparent substrate serves additionally as a spacer and produces with the mask an interference pattern in the resist which causes very porous side wall structures.

different molecules: first Octadecanethiol (ODT) for gold (Au) surfaces and 3,3,4,4,5,5,6,6,7,7,8,8-Tridecafluorooctyl-triethoxysilan (DYNASYLAN<sup>®</sup>) for titanium oxide (TiO) surfaces. The functionality of DYNASYLAN<sup>®</sup> as self assembled monolayers has been reported elsewhere [13]. The coating was done by dip coating from 0.5 M solutions of ODT and DYNASYLAN<sup>®</sup>, followed by a heating step of 70°C for 10 minutes.

The contact angle experiments were carried out with the EASYDROP-Standard model from Krüss GmbH, Hamburg. The advancing contact angle experiments were done by placing a 2  $\mu\text{L}$  drop on the surface and increasing the volume to 10  $\mu\text{L}$  with the needle remaining in the drop. The receding contact angle experiments were done the opposite way starting by 10  $\mu\text{L}$  and decreasing the volume to nearly 2  $\mu\text{L}$ . The measurement was carried out and plotted automatically. The angles were determined by calculating the average values from the horizontal section of the plotted graphs.

### 4 EXPERIMENTAL DETAILS

The results of the lithographic procedure are shown in Figure 2 and 3. Due to the setup utilizing backside exposure and a thick transparent substrate acting both as spacer and additional UV filter, the pattern transfer from the mask is strongly deteriorated and thus structures with tilted side walls can be generated (proximity exposure).

#### 4.1 Structured SU 8

Figure 2 shows a variation of the exposure dose from 50 (picture 1) to 300 (picture 6) mJ/cm<sup>2</sup> through a mask with square structures of 12  $\mu\text{m}$  width and a distance of 40  $\mu\text{m}$  between the patterns. As one can see, the structures broaden when the dose is increased until they finally merge together. Result of this is an increasing contact area between the drop and SU 8, while the contact to the substrate is decreased. Simultaneously the contact angle increases to values of nearly 125°.

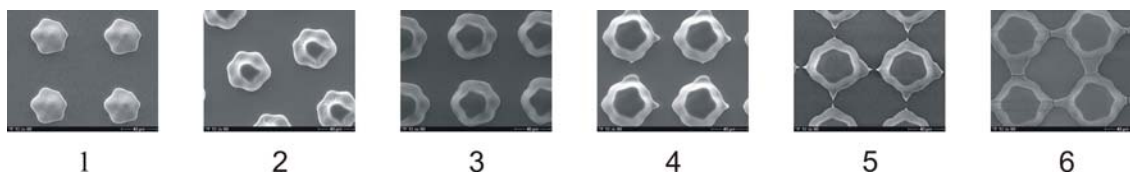


**Figure 2:** Dose variation from 1 to 6 ranging from 50 – 300 mJ/cm<sup>2</sup> of 12 μm SU 8 structures and a distance of 40 μm.

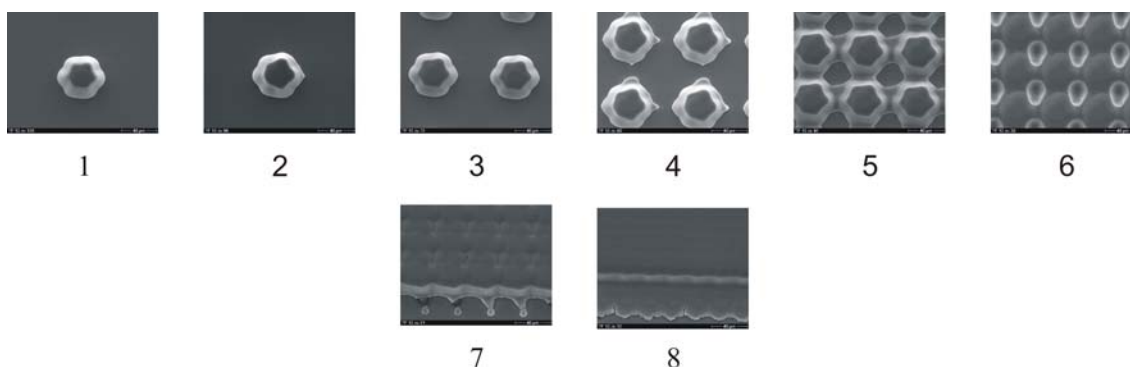


**Figure 3:** Distance variation from 1 to 8 ranging from 120 – 12 μm with a constant dose of 200 mJ/cm<sup>2</sup> and a SU 8 structure width of 12 μm.

Figure 3 shows a pattern of 12 μm square structures with different distances ranging from 12 μm to 120 μm all exposed with a constant dose of 200 mJ/cm<sup>2</sup>. The contact angles (ca) measured on such surfaces without an additional coating, are given in table 1.

Assuming from the large hysteresis (hys.) of all structures, the Wenzel-state is preferred by wetting those surfaces. There is an increasing contact angle for the structures when the spaces between them are decreasing. The maximum of the non wetting behavior is reached with a structure distance on the mask of 60 μm (see figure 3.4 and 2.4). For shorter distances the wettability of the surface is mainly influenced by the glass (contact angle around 70°). For bigger distances the contact angle is determined by the characteristics of the SU 8. But if the structure network becomes more dense, the resist forms smooth planes like shown in figure 3.7 and 3.8. and the contact angle

| structure width [μm]     | structure distance [μm] | ca [°] | hys. [°] |
|--------------------------|-------------------------|--------|----------|
| 12                       | 120                     | 88     | 64       |
| 12                       | 96                      | 91     | 77       |
| 12                       | 72                      | 86     | 70       |
| 12                       | 60                      | 125    | 100      |
| 12                       | 42                      | 103    | 86       |
| 12                       | 30                      | 86     | 47       |
| 12                       | 21                      | 83     | 41       |
| 12                       | 12                      | 85     | 39       |
| SU 8 with flash exposure |                         | 88     | 44       |

**Table 1:** Overview of contact angles (ca) on patterned SU 8 surfaces. The standard deviation of all contact angles is less than ± 3°.

decreased to values of plane SU 8. To increase the non-wetting behavior, the SU 8 surfaces can easily be coated with thin metal films which serve as adhesion layer for different self assembled mono layers and cause further surface tension reduction.

## 4.2 Coating with SAM

In this part we used ODT together with a 50 nm Au-layer and DYNASYLAN<sup>®</sup> together with an 800 nm TiO-layer. Structures shown in figure 3 were coated with these SAM-metal-films and the contact angle results are shown in table 2.

The wetting behavior of the SU 8 structures can be increased dramatically by both coating techniques, whereas

| structure width [μm]       | structure distance [μm] | ca [°] | hys. [°] | ca [°]   | hys. [°] |
|----------------------------|-------------------------|--------|----------|----------|----------|
|                            |                         | Au-ODT |          | TiO-DYNA |          |
| 12                         | 120                     | 122    | 29       | 165      | 11       |
| 12                         | 96                      | 162    | 17       | 163      | 16       |
| 12                         | 72                      | 163    | 29       | 162      | 16       |
| 12                         | 60                      | 162    | 33       | 162      | 19       |
| 12                         | 42                      | 146    | 45       | 163      | 26       |
| 12                         | 30                      | 123    | 22       | 160      | 35       |
| 12                         | 21                      | 113    | 12       | 159      | 60       |
| 12                         | 12                      | 114    | 13       | 161      | 47       |
| Au-ODT                     |                         | 112    | 13       |          |          |
| TiO-DYNASYLAN <sup>®</sup> |                         |        |          | 150      | 60       |

**Table 2:** Overview of contact angles on structured SU 8 surfaces covered with two different metal thin films and self assembled mono layers. The standard deviation of all contact angles (ca) is less than ± 3°.

the changes caused by the TiO film are more effective. This is because DYNASYLAN<sup>®</sup> on a titanium oxide surfaces ( $R_a \sim 90$  nm) is already ultra-hydrophobic with a contact angle of around  $150^\circ$ . The following macro roughness produced by the SU 8 structures has not a big influence on the contact angle itself but the hysteresis can be reduced dramatically to values of  $11^\circ$ . These results predict that the drops on such surfaces are in the “fakir state” and do not penetrate the space between them.

The same behavior could be observed for the Au-ODT surfaces with hysteresis of around  $30^\circ$ . Although these results are very promising for droplet transportation experiments, the hysteresis is still too high for that.

### 4.3 Reduced exposure dose

In this section we used the same mask as before but reduced the exposure dose to below  $50 \text{ mJ/cm}^2$ . That means we were working very close to the threshold dose of SU 8. Below these values one can hardly see a cross linking effect at all. For practical reasons, the resist thickness was increased above the desired thickness of finished structures. With these exposure conditions, we could make sure that the propagated light was totally absorbed within the resist layer. The results are shown in figure 4 and 5.

The SU 8 structures can be modified in a way that the whole structures become very porous and show a very strong non-wetting behavior. For structures and surfaces like this coated with TiO-DYNASYLAN<sup>®</sup> thin films, we could achieve contact angles of  $165^\circ \pm 2^\circ$  with a hysteresis of only  $5^\circ$ . Furthermore, with decreasing structure width on the mask one can achieve nearly flat surfaces with nano porous properties (figure 5). Such surfaces can be easily integrated into fluidic structures by multi step exposures.

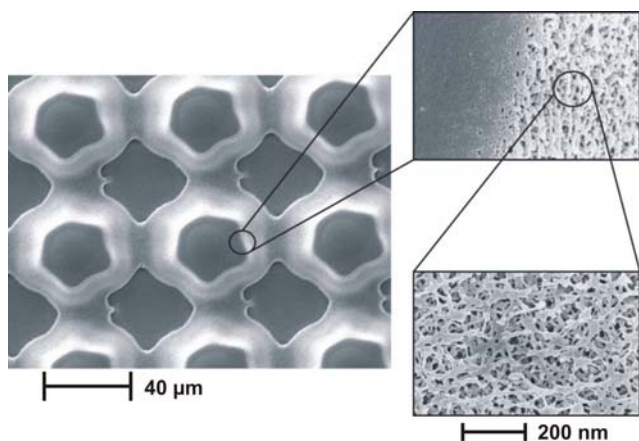


**Figure 4:** The detail view of an plant-like structure with very porous side walls.

## 5 CONCLUSION

Using a modified UV exposure technique utilizing a special mode of backside exposure, we are able to generate hydrophobic structures consisting solely of SU 8. The

additionally coated thin metal films act as an adhesion layer for different self assembled monolayers, thus leading to ultra-hydrophobic structures with very low contact angle hysteresis. The structures fabricated this way provide all necessary qualities for the application in surface tension generated drop transportations and can be prepared using a very easy lithographic procedure.



**Figure 5:** A nearly flat surface made by back-side exposure with nano pores below 500 nm.

## 6 OUTLOOK

The nano porous structures are going to be used in EWOD (electro wetting on dielectric) processes as dielectric layer and as ultra-hydrophobic surfaces for providing the drop form of the fluids. Furthermore, there are projects in preparation for using the nano porous flat surfaces as nano membranes for gassing and mass transfer procedures in micro fluidics.

## REFERENCES

- [1] Cerman, Z. et al., *Biol. Unserer Zeit*, **2004**, 34, 290-296
- [2] Yoon, J.-Y., Garrell, R.L., *Anal. Chem.*, **2003**, 75, 5097-5102
- [3] Squires, T.M., Quake, S.R., *Reviews of modern physics*, **2005**, 77, 977-1026
- [4] Brochard, F., *Langmuir*, **1989**, 5, 432-438
- [5] Subramanian, R.S. et al., *Langmuir*, **2005**, 21, 11844-11849
- [6] Chaudhury, M.K., Whitesides, G.M., *Science*, **1992**, 256, 1539-1541
- [7] Moumen, N. et al., *Langmuir*, **2006**, 22, 2682-2690
- [8] Petrie, R.J. et al., *Langmuir*, **2004**, 20, 9893-9896
- [9] Lü, C. et al., *Sensors and Actuators A*, **2006**
- [10] Yoon, Y.-K. et al., *J. of Micro-Electromechanical Systems*, **2006**, 15, 1121-1130
- [11] Wenzel, R.N., *Industrial and Engineering Chemistry*, **1936**, 28, 988-994
- [12] Cassie, A.B.D., Baxter, S., *Trans. Faraday Soc.*, **1944**, 40, 546-551
- [13] Schondelmaier, D. et al., *Langmuir*, **2002**, 18, 6242-6245